Tellus (1990), *42A*, 246–258

A case study of marine cyclogenesis near Cape Town

By MARK JURY, *Oceanography Department, University of Cape Town, Rondebosch, 7700, South Africa* and MIKE LAING, *South African Weather Bureau, PB X097, Pretoria, 0001, South Africa*

(Manuscript received 8 August 1988; in final form 4 April 1989)

ABSTRACT

A case study of southern hemispheric marine cyclogenesis near Cape Town is examined using surface and upper air observations and satellite imagery. The mesoscale cyclone formed in the cold air mass behind a larger trough and deepened by 8 hPa over a 6-h period. Simultaneously, the system increased in speed from 12 to 24 m s^{-1} as determined by satellite tracking of the comma cloud mass. NOAA 10 and Meteosat enhanced infrared imagery provided insight into the structure of convection and indicated a dry slot being advected into the vortex from the equatorwards side of the occluding low. Cyclogenesis coincided with passage of the warm sector over the edge of the Agulhas Current. Surface heat fluxes of 200 W m^{-2} were sustained across the warm sector, sharpening the upper air ridge preceding the trough. In addition to surface inputs of energy, synoptic scale and baroclinic forcing of the system was conducive to cyclogenesis. At the 250 hPa level, maximum divergence and vorticity values approached 10^{-4} s^{-1}, just west of the area of surface cyclogenesis. At the 850 hPa level, the temperature and streamline fields aligned in a small area to the southwest of Cape Town, providing an estimated thermal wind of 20 m s^{-1} over the 1000–700 hPa layer. Following the passage of the vortex, a meso-high/gust front produced surface winds of 49.1 m s^{-1} along the coast. Other aspects of the mesoscale circulation are presented from a network of surface weather stations near Cape Town.

1. Introduction

Rapidly developing, mesoscale cyclones in middle and high latitudes have recently become the focus of research both from the point of view of the processes involved (Reed, 1979; Rasmussen, 1979) and the forecasting implications (Browning and Monk, 1982; Sanders, 1986). These storms are most frequent in the early winter (Murty et al., 1983) due to the differential seasonal cooling of the ocean relative to the overlying atmosphere. Explosively developing lows are typically less than 500 km in diameter and contain surface wind speeds of more than 30 m s^{-1} (Shapiro et al., 1987). Remotely sensed and intensive project data sets on the rapid marine cyclogenesis over warm western boundary currents such as the Gulf Stream (Davis and Emanuel, 1988) have stimulated interest in this subject.

Prior to the advent of satellite technology and fine mesh synoptic model analyses, weather forecasters relied on sparse observations from ships and coastal stations. In the post-war period, the notion of a weak perturbation developing when cold air overflowed warmer water was widely held. However, this argument for purely thermal enhancement by surface heat fluxes over open seas was already in question by the late 1960s (Harrold and Browning, 1969). Mansfield (1974) suggested that these meso-lows were the result of baroclinic instability being trapped within a weakly stratified marine boundary layer. Reed (1979) proposed that a deeper layer needed to become baroclinically unstable on the equatorward side of the upper jet core. Rasmussen (1979) showed that meso-lows in the higher latitudes could be initiated by cumulus convection through the process of Conditional Instability of the Second Kind (CISK). More recent work by

Emanuel (1986) and Davis and Emanuel (1988) have indicated that the CISK mechanism plays a smaller role in relation to the more direct influence of the sensible heat input at the air–sea interface.

Bratseth (1985) found that the moisture convergence in the marine boundary layer was proportional to the geostrophic vorticity. These ideas were further investigated by Danard (1986) who indicated that lows moving over water warmer than 18 °C could experience a sensible heat increase to 350 W m^{-2}. Following a period of adjustment, moisture convergence in the boundary layer led to predictions of precipitation rates above 40 mm h^{-1}.

A number of other investigators, Businger (1985) and Rogers and Bosart (1986) for example, have suggested that upper level baroclinic forcing triggered the initial development of the meso-low. The latter authors performed a composite analysis and found that upper level flow should be diffluent on the downstream side of the surface low. In an analysis of cyclogenesis off Cape Hatteras, Sanders (1986) found an acceleration in the upper trough/surface low from 15 m s^{-1} to over 20 m s^{-1} associated with increasing baroclinicity. In such cases of cyclogenesis, the upper trough contained a cyclonic vorticity maximum of order f located about 500 km to the west of the area of surface cyclogenesis. Another common attribute of cyclogenesis is a jet streak on the leading edge of the upper trough (Callaghan, 1987).

Businger (1987) discussed the climatology of polar lows which form as secondary waves in the cold air trailing behind a leader trough. He distinguished between the larger comma cloud and the smaller spiralling vortex containing a cloud-free center. Many of these systems develop in the high latitudes to the north of 50° N during the winter season when Arctic air masses move off the ice sheets near the coasts of Alaska and Greenland and over relatively warmer waters fed by the Kuroshio and Gulf Stream Currents (Rasmussen, 1985). Clearly these polar lows differ from their mid-latitude counterparts in some respects (Rasmussen and Zick, 1987); however, it is the intention here to show that the meso-low which developed near Cape Town (Fig. 1) exhibits many of the attributes of the polar low as outlined by Auer (1987).

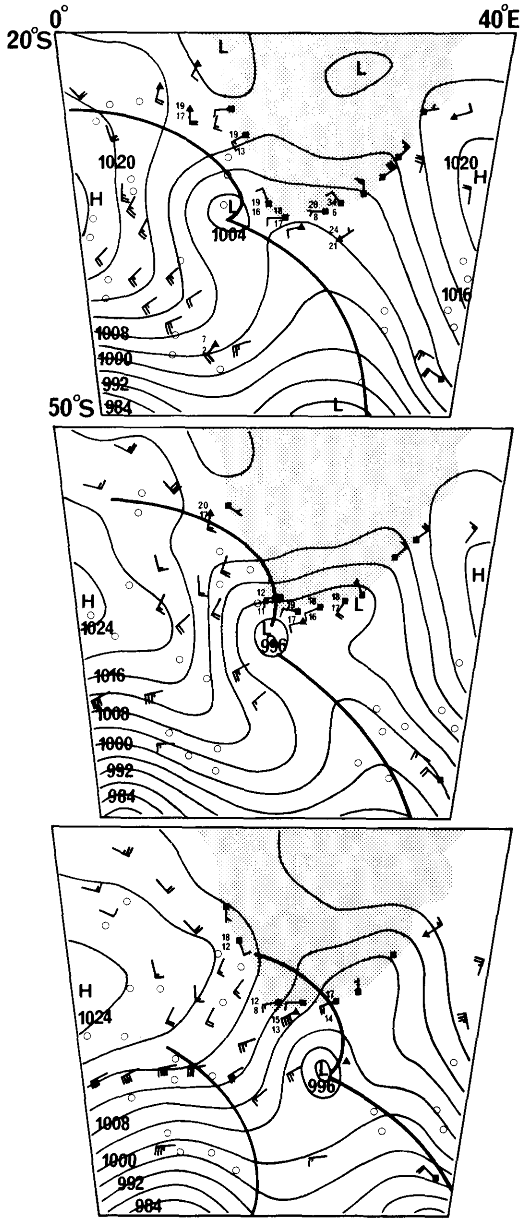

Fig. 1. Surface pressure analysis for 14.00 hrs, 4 May 1987 (top); 20.00 hrs, 4 May (middle); and 02.00 hrs, 5 May (bottom), showing the development and movement of a surface low. Isobars are analysed every 4 hPa. Squares represent coastal reports, triangles—ships and circles—buoys. Satellite winds over the oceans are represented by wind barbs in the conventional fashion. The southwestern-most coastal station is Cape Town. The continent is shaded. Map borders are 20–50°S, 0–40°E here and in Fig. 4.

In the early winter month of May, the southern hemisphere jet-stream often accelerates in response to a growing meridional temperature gradient. Initially the jet stream may have a low zonal index containing large amplitude Rossby waves which meander out of the higher latitudes. Westerly perturbations, sweeping the southern oceans in a circumpolar fashion, are then guided equatorwards and may propagate across warm ocean currents such as the Agulhas to the south of Africa. The subsequent input of heat energy to the incipient cyclone may trigger explosive cyclogenesis (-1 hPa h^{-1}) if supported by upper forcing. This baroclinic forcing is primarily dependent on the meridional temperature gradient and vertical shear of the zonal wind through the troposphere. On the polewards side of the Agulhas Current (near 40°S, 20°E), meridional sea surface temperature gradients approach 10°C 10 km^{-1} (Gilloly and Walker, 1984) and so the baroclinicity of upper troughs is enhanced. To the south of Africa, these westerly waves become fast-moving and consequently the blocking index is low (Australian Bureau of Meteorology, 1987). To the east of this region, in middle and high latitudes of the southern hemisphere, upper troughs accelerate eastwards and intensify (James, 1983 and Wallace, 1983).

The relative importance of upper forcing and surface flux inputs to the process of cyclogenesis is addressed in the case study presented. In addition to investigating the controlling processes of cyclogenesis near Cape Town, the pattern recognition problem is addressed. In order to forecast the development of meso-lows, model analyses typically utilize the release of potential energy through baroclinic processes as the main driving mechanism. Thus the initial values need to be well specified by observations, a substantial problem in the data sparse southern oceans to the south of Africa.

2. Data

The case study data set includes the ECMWF synoptic model initializations at 02.00 hrs, 4 May 1987 of the 250 hPa and 850 hPa level winds and temperatures to define the precursor stage. All times quoted refer to local time or UTC + 2 h. An ECMWF 500 hPa hemispheric analysis of geopotential heights for 02.00 on 5 May 1987 is used to illustrate the large scale circulation features in relation to the mesoscale cyclone. S. A. Weather Bureau synoptic surface maps for 14.00 and 20.00 on 4 May and 02.00 on 5 May 1987, and 700 and 300 hPa levels charts for 14.00 on 4 May and 02.00 on 5 May give a detailed perspective of the cyclogenesis stage. These were objectively analysed from land, ship, and buoy reports and satellite winds and TOVS thicknesses. Meteosat and NOAA 10 infrared images are used to study the structure of the meso-low at the point of cyclogenesis. Sea surface temperature (SST) data near Cape Town were obtained by compositing commercial ships data over the period 20 April–10 May 1987 with NOAA 9 AVHRR infrared imagery for two relatively cloud free days: 21 and 29 April 1987. The ships data were confined to the shipping lane within 200 km of the coast to the south and southeast of Cape Town, but spread further seawards off the west coast. Routine three hourly surface observations of winds, pressure, temperature, clouds, etc. and vertical radiosonde profiles for Cape Town at 14.00 and 02.00 were extracted from the S. A. Weather Bureau data bank. To investigate the mesoscale structure of the coastal circulation systems over the period of cyclogenesis, surface data from a network of weather stations in the vicinity of Cape Town were utilized. Together these data provide a perspective of the storm as it skirted the southwestern tip of Africa. The lack of additional information over the marine areas to the south of Africa for this case study and others similar to it, limits our interpretation and continues to plague the prediction and research of marine cyclogenesis in the wider context of the southern hemisphere.

3. Precursor stage and synoptic setting

The sequence of events was initiated by the movement and sharpening of a wave of length 6960 km in the region to the southwest of Africa as indicated by the ECMWF 500 hPa southern hemispheric initialization for 02.00, 5 May 1987 in Fig. 2. The trough in the high- and mid-latitudes (dashed line) in relation to the path of cyclogenesis (dots) tilted gradually forward through the period of cyclogenesis, indicating the

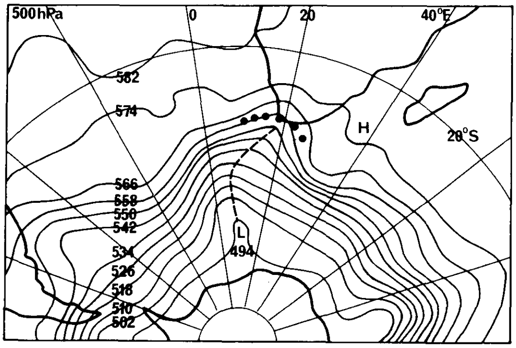

Fig. 2. ECMWF 500 hPa hemispheric analysis illustrating geopotential contours at 80 gpm intervals at 02.00, 5 May 1987. The trough is represented by the dashed line. 6-hourly positions of the surface low are shown by dots from 02.00 4 May to 08.00 5 May 1987. The upper ridge to the SE of Africa and the high-latitude low are labelled.

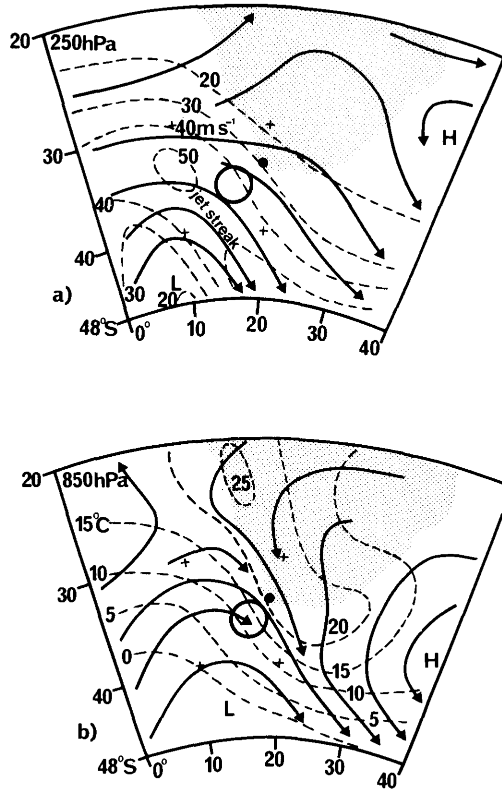

Fig. 3. (a) ECMWF 250 hPa initialization for 02.00, 4 May 1987 showing the wind streamlines and isotachs (dashed, m s^{-1}). The jet streak is labelled. (b) ECMWF 850 hPa initialization as in (a) showing wind streamlines and isotherms (dashed, °C). The open circle denotes the area of cyclogenesis. Cape Town is shown by the dot.

formation of a shorter and faster-moving secondary wave on the trough's equatorwards side. The 500 hPa trough was fairly symmetric in the high latitudes but considerably kinked on its eastwards edge in the mid-latitudes. Sharpening of the leading edge of the trough by a quasi-stationary ridge over the Agulhas Current region was noted. The high-latitude cyclone moved eastwards and equatorwards across the eastern South Atlantic from 58°S, 28°W (984 hPa) through 54°S, 02°W (974 hPa) to 52°S, 10°E from 02.00 3 May to 02.00 5 May 1987. Satellite imagery verified the surface low to be near 57°S, 07°W at 02.00 on 4 May. By 14.00 4 May the 500 hPa height at Cape Town had dropped from 5820 to 5680 gpm.

The ECMWF initialization at 02.00 4 May 1987 for the 250 and 850 hPa levels (Fig. 3a, b) illustrates the spatial structure of the precursor stage. The sharpness of the trough is evident. Wind streamlines curved cyclonically by 110° in the 40–48°S latitude zone, across the longitudes 0–20°E. 250 hPa winds were over 50 m s^{-1} in a narrow band to the southwest of Cape Town, constituting a jet streak on the front edge of the upper trough. A significant diffluence of the upper wind streamlines on reaching the west side of the African continent was noted. The upper ridge situated to the southeast of Africa near 30°S, 35°E (Figs. 2–4), was largely responsible for the diffluence, a precursor pattern recognized by Rogers and Bosart (1986). We use standard resolution wind data from the ECMWF model to calculate the 250 hPa divergence over the area 30–40°S, 10–20°E to the southwest of Cape Town. A value of $+1.8\ 10^{-5}\ s^{-1}$ was estimated. The vorticity, evaluated about 500 km to the southwest of the area of surface cyclogenesis as suggested by Sanders (1986), was $-6.9\ 10^{-5}\ s^{-1}$, in agreement with values extrapolated from Sardie and Warner (1983) for "dry" cyclogenesis. These upper level positive divergence and cyclonic vorticity values, while computed at a relatively coarse resolution, indicate that sufficient baroclinic forcing was present to trigger a sub-synoptic scale vortex. At the 850 hPa

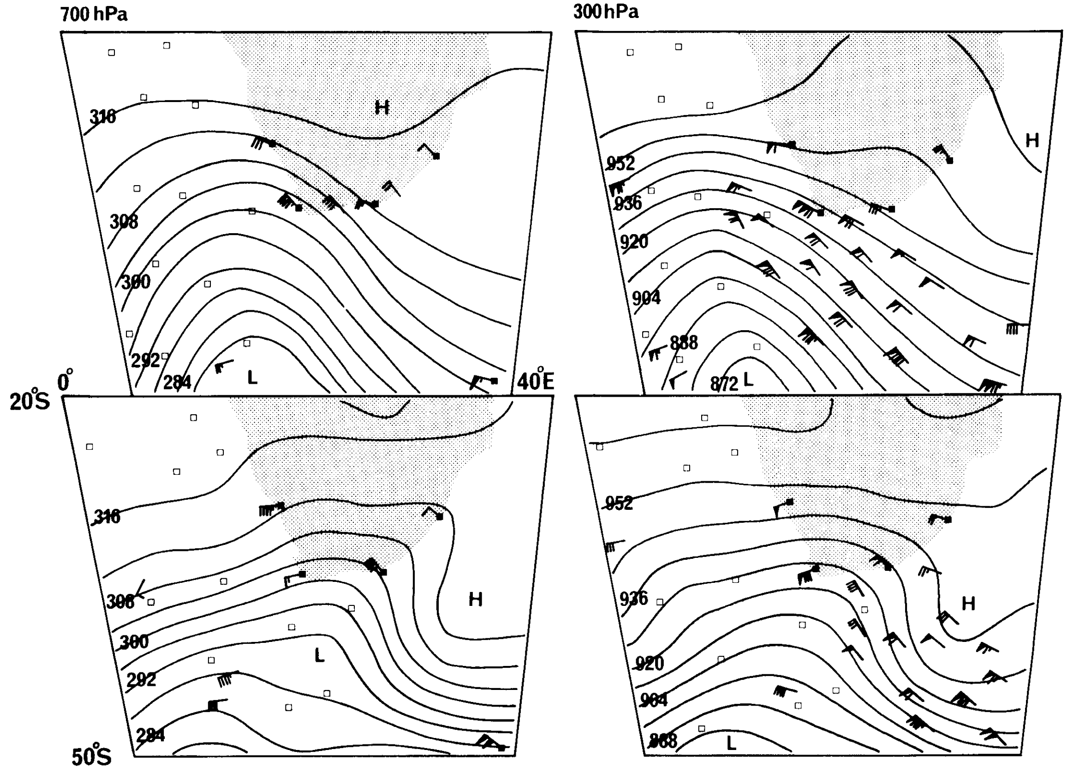

Fig. 4. Geopotential contours objectively analysed for the 700 hPa (left) and 300 hPa (right) levels at intervals of 40 gpm and 80 gpm, respectively. The top maps are for 14.00, 4 May 1987, while the bottom correspond to 02.00, 5 May 1987. Coastal radiosonde data are denoted by squares, TOVS thicknesses by open squares and satellite winds by barbs as in Fig. 1.

level, wind streamlines and isotherms from the ECMWF model initialization for 02.00, 4 May 1987 were analysed to investigate atmospheric forcing near the top of the marine boundary layer. Fig. 3b shows that the streamlines were rather convergent at the 850 hPa level to the southwest of Cape Town. Flow trajectories followed the west coast from as far north as 20°S. Along this west coast axis, the isotherms were also aligned such that a baroclinic low level jet resulted. Such a meridional inflow in the surface layer has been documented as a necessary precondition for explosive cyclogenesis (Gyakum, 1983; Reed and Albright, 1986; Bosart, 1981; Davis and Emanuel, 1988). Considering that a 10°C horizontal temperature gradient (oriented SW–NE) could likely be maintained through the lower troposphere, the thermal wind relationship provides an estimated 20 m s^{-1} increase in the meridional wind speed from the surface to the 700 hPa level. In Fig. 5 this result is verified by the Cape Town radiosonde profile. On either side of the 850 hPa thermal wind axis, air of differing properties converged. To the east, subtropical Agulhas Current-influenced air was in circulation with average temperatures of over 15°C at the 850 hPa level. To the southwest over the South Atlantic, sub-zero air of mid-latitude origin was advected towards the west coast axis. Using ECMWF wind inputs, we estimate 850 hPa convergence and vorticity values of $-0.43\ 10^{-5}$ s^{-1} and $-0.75\ 10^{-5}$ s^{-1}, respectively. Again it can be seen that the traditional synoptic scale baroclinic mechanisms of low-level convergence and cyclonic vorticity were present in the precursor stage of the storm's lifecycle. Comparing the 850 hPa

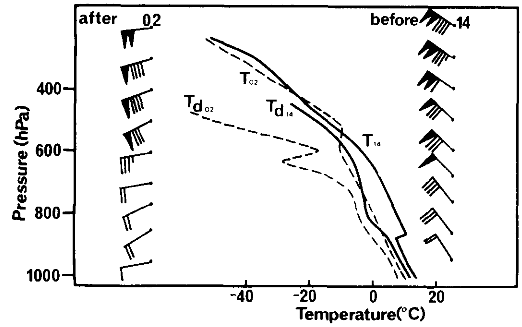

Fig. 5. Cape Town radiosonde profiles for 14.00, 4 May 1987 and 02.00, 5 May 1987 showing winds at the standard levels, and temperature and dewpoint profiles (14.00—solid and 02.00—dashed), plotted linearly from 1000 to 200 hPa.

and 250 hPa trough axes (Figs. 3a and b), a tilt of about 600 km is found and can be considered suitable for baroclinic development.

The 850 hPa horizontal temperature field arising from heating over the African plateau and extended polewards by the warm Agulhas Current, therefore had a significant impact on the synoptic scale setting and baroclinic forcing. For a brief period, the temperature wave in the atmosphere and ocean (a spatially anchored, climatological condition (Newton, 1972; Holflich, 1984)) matched the transient upper wave dimensions and created a positive feedback mechanism for cyclogenesis. In numerical simulations Nuss and Anthes (1987) and Atlas (1987) have shown that a sinusoidally varying SST front, when temporarily matched by an atmospheric wave of similar dimensions, promotes the process of cyclogenesis through the preferential supply of heat into the warm sector of the storm system. Hence, the positioning of the surface fluxes relative to the storm is more important than the magnitude of the fluxes. In Section 4, we trace the structure, evolution and processes governing the meso-low and analyse the spatial distribution of the fluxes over the warm sector of the storm.

4. Cyclogenesis

On 3 May at 20.00 hrs, a cold front was passing 36°S, 07°E with no evidence of wave development or cyclogenesis in the cold rear sector. By 02.00 on the 4 May, satellite imagery indicated the development of a weak wave near 36°S, 11°E with a central pressure of 1008 hPa. Surface pressure analyses of the developing system from 14.00 on 4 May to 02.00 on 5 May, shown in Fig. 1, revealed a sudden drop in central pressure from 1004 hPa at 14.00 (according to drifting buoy data) to 996 hPa at 20.00 (as estimated from gradient wind balance). At the upper levels, the geopotential fields during cyclogenesis (Fig. 4) indicated the eastwards displacement and cyclonic rotation of a sharp trough. Observed and satellite derived winds of 40 m s^{-1} characterized the leading edge of the trough at the 300 hPa level at 14.00 (top right). Winds were significantly higher at Cape town than elsewhere, confirming the results of Fig. 3a, that a cyclonic vorticity maximum was located just to the southwest of Cape Town. The trough amplitude flattened with time but a ridge to the southeast of Africa (seen in the lower panels of Fig. 4) maintained the sharpness of the upper trough as it tracked eastwards. It can be noted that the TOVS and satellite wind data were suitably located to improve confidence in the analysed structure.

Positions of the mesoscale cyclone for the period 02.00 4 May to 02.00 5 May are shown in Fig. 2, and in Fig. 6 superimposed onto a composite SST analysis. The meso-low crossed 16°E at a speed of about 12 m s^{-1}. At this time the vortex encountered significantly higher SSTs over the Agulhas Current (24°C). Off the west coast, SSTs were over 22°C and in general anomalies were about 2°C above the autumn climatological mean. We may crudely estimate the input of heat from the ocean to the atmosphere using the bulk aerodynamic formulae for sensible and latent heat of Friehe and Schmitt (1976). We take the air density to be 1.2 kg m^{-3} and the exchange coefficients for sensible and latent heating to be 1.1 10^{-3} and 1.3 10^{-3}, respectively. The surface wind speed was inferred from the observed winds and pressure gradients in Fig. 1. Air temperature and dewpoint values were interpolated from nearby ship, island and coastal data. Together with the SSTs from Fig. 6, the vertical gradients of temperature and moisture could be computed. Table 1 shows the interpolated data and the spatial distribution of the fluxes in relation to the meso-low at 36°S, 15°E.

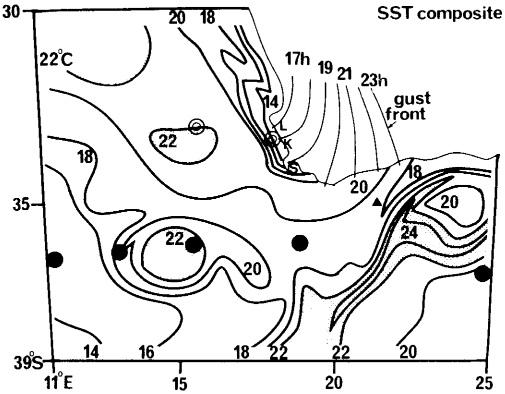

Fig. 6. Sea surface temperatures (SST) using composited ship and satellite data, subjectively analysed every 2°C. SSTs over 22°C are shaded. The 6-hourly position of the low is shown by the dots from 02.00, 4 May 1987 to 02.00, 5 May 1987. Meso-high positions at 15.00 and 20.00 are indicated by the open circles. Coastal weather stations used to describe the mesoscale environment are shown by the letters L, K and S. The oil rig is shown by the triangle. The hourly position of the gust front is illustrated by the thin line over the land.

Table 1 shows that upwards heat fluxes were well distributed over the warm sector of the mesoscale cyclone just prior to the time of cyclogenesis. Highest heat fluxes (487 W m^{-2}) occurred over the warm eddy at 36°S, 15°E. The ratio of sensible to latent heating was about 1:4 and can be attributed to the marine wind fetch and high SSTs near Cape Town. The heat flux integrated over the area of the warm eddy was of order 10^{13} W, suggesting that the eddy, together with the fluxes over the Agulhas Current significantly improved conditions for low level instability and mesoscale cyclogenesis. At the synoptic scale, the matching of the atmospheric and oceanic temperature patterns, (compare Figs. 3b and 6) similarly contributed to enhanced baroclinicity. Rapid eastward movement of the system and surface convergence brought warm Agulhas air beneath the preceding ridge (Fig. 4, bottom), sharpening the trough and the upper vorticity advection. It can be noted that along the south coast ahead of the leader front, latent heat fluxes of order 400 W m^{-2} were made possible by dry plateau level winds flowing seawards across

Table 1. *Spatial distribution of heat fluxes at 14.00 hrs, 4 May 1987*

Longitude / Latitude	15°E				17°E				19°E				21°E			
32°S	SST	21	T	18	SST	17	T	18	coast				coast			
	T_d	14	U	14	T_d	14	U	14								
	Q_h	55	Q_e	300	Q_h	19	Q_e	135								
	Q_T	355			Q_T	117										
34°S	SST	21	T	16	SST	20	T	18	coast				coast			
	T_d	15	U	16	T_d	16	U	20								
	Q_h	90	Q_e	312	Q_h	48	Q_e	273								
	Q_T	402			Q_T	321										
36°S	SST	22	T	15	SST	19	T	17	SST	19	T	19	SST	24	T	24
	T_d	10	U	11	T_d	14	U	06	T_d	16	U	04	T_d	18	U	08
	Q_h	102	Q_e	385	Q_h	16	Q_e	82	Q_h	00	Q_e	109	Q_h	00	Q_e	203
	Q_T	487	*		Q_T	98			Q_T	97			Q_T	203		
38°S	SST	16	T	12	SST	18	T	16	SST	23	T	18	SST	21	T	20
	T_d	08	U	11	T_d	12	U	05	T_d	14	U	05	T_d	16	U	06
	Q_h	58	Q_e	193	Q_h	13	Q_e	78	Q_h	33	Q_e	146	Q_h	08	Q_e	129
	Q_T	251			Q_T	110			Q_T	179			Q_T	137		

Values are given for sea surface temperature (SST), air temperature (T), dewpoint temperature (T_d) in °C and 10 m wind speed (U) in m s^{-1}. Sensible (Q_h), latent (Q_e) and total (Q_T) heat fluxes in W m^{-2} are estimated. The meso-low is denoted by *.

the warm current (see Fig. 1, top, coastal station where T_d dep = 28 °C). Unfortunately further analysis of heat flux derivatives are precluded by the poorly specified initial field.

For cases of polar lows, Businger (1987) has estimated a tropospheric response lag of 2 h to an input of 324 W m^{-2} of sensible heat. While the sensible heat flux for cyclogenesis downstream of a continent or ice mass is typically larger, the addition of latent heating for the case presented here provides a similar order of magnitude for the heat fluxes and we would expect a similar tropospheric response lag. Assuming that these heat flux conditions could be maintained over the 6-h period during which cyclogenesis took place (14.00–20.00, Fig. 1), we obtain a time-integrated flux value of order 10^7 J m^{-2}, similar to that reported by Buzzi and Speranza (1983) from an energy budget calculated for cyclogenesis over the northern Mediterranean.

The intensity of the lower tropospheric energy flux is further quantified using Auer's (1987) modified polar low index, the difference between the 700 hPa temperature and the SST. For our case of the low over 22°C water and taking the 700 hPa temperature at Cape Town prior to and following the passage of the storm (4 and −6 °C, respectively), differentials of 18 °C in the warm sector and 28 °C in the cold sector were found. This ranks with Auer's strong polar low cases over the Tasman Sea which exhibit SST—700 hPa T differentials of over 26°C. The sequence of cyclogenesis then unfolded as the warm sector of the low came into contact with the warm waters of the Agulhas Current at 14.00. The central pressure deepened from 1004 hPa to

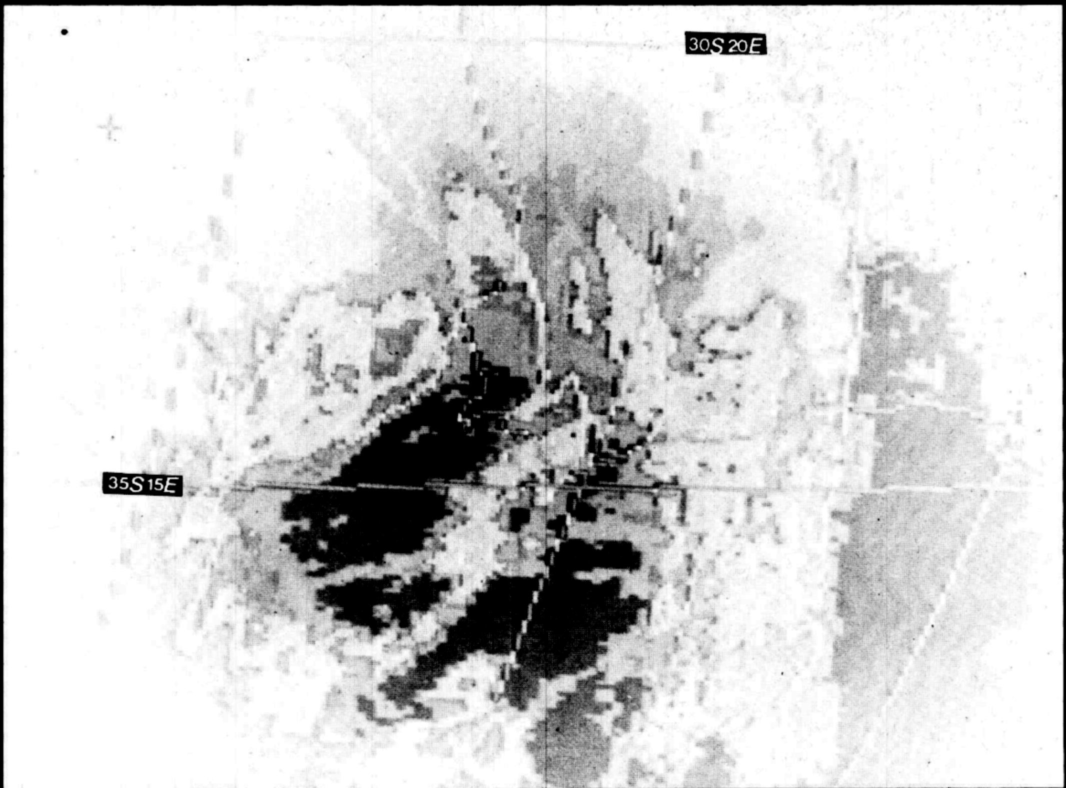

Fig. 7. Meteosat McIdas-enhanced infrared cloud analysis at 20.00, 4 May 1987. Coldest clouds are lightest grey, warmer clouds are darker grey. A multiple vortex pattern is evident. The leader front is followed by a secondary wave and the vortex/dry slot over Cape Town.

996 hPa as the vortex accelerated from 16°E to 19°E over the next 6 h. The pressure tendency following the low exceeded -1 hPa h^{-1} and its speed of movement doubled to 24 m s^{-1}, in agreement with the case of Sanders (1986).

Satellite imagery indicated that the (inverted) comma cloud mass was located between 11 and 15°E at 14.00 on 4 May. Concurrently with the rapid cyclogenesis, a dry slot of air became entrained into the system from the equatorwards sector (shown by the double circle in Fig. 6 at 17.00 and 20.00). Surface data suggested that the dry slot represented a mesoscale high pressure cell following rapidly in on the developing surface low. The leader front, secondary wave and vortex/dry slot can be seen in the Meteosat and NOAA 10 infrared images for 20.00 and 21.00, 4 May 1987, in Figs. 7 and 8, respectively. The leader front had passed 23°E and the developing vortex/dry slot was located near 36°S, 19°E and moving in an east-southeast direction. Such a multiple vortex structure is similar to that noted by Businger and Walter (1988) and Locatelli et al. (1982). These images identify considerable detail in the convective structure and highlight the rapid occlusion process in the NE–SW orientation of the comma cloud. Its zonal and meridional extent during cyclogenesis was

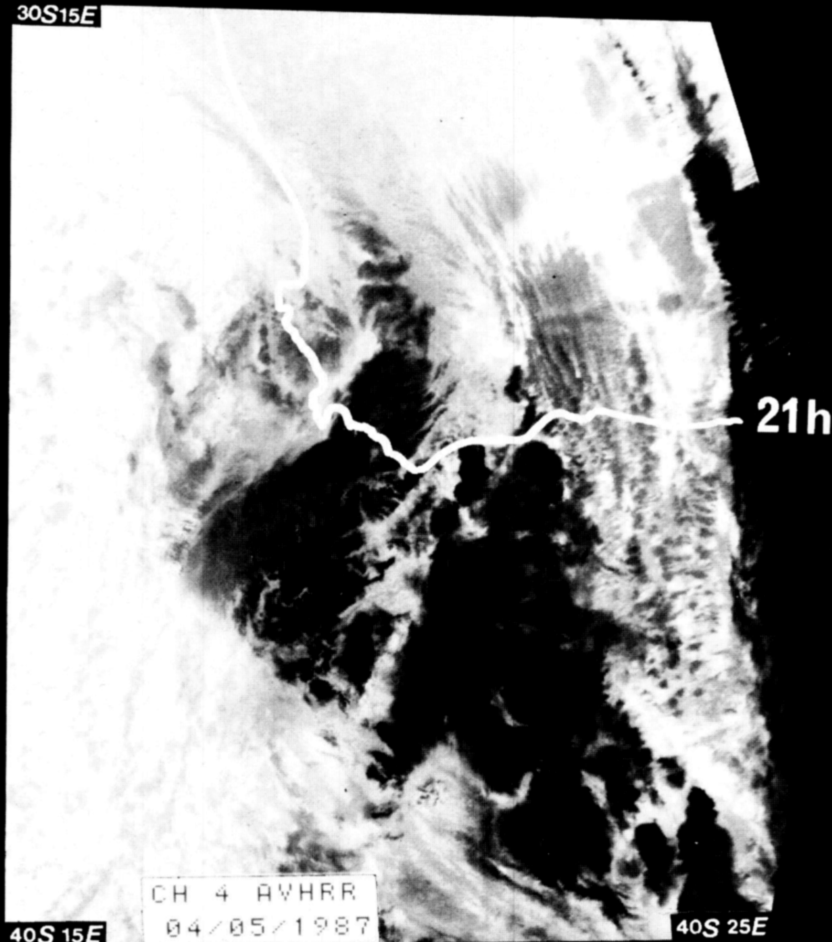

Fig. 8. NOAA 10 infrared image of the cyclone obtained at 21.00, 4 May 1987. The NOAA image borders are 30–40°S, 15–25°E.

400 × 500 km. Agee and Lidrbauch (1989) show that this type of cloud structure is more typical for baroclinically induced North Pacific storms, less dominated by convective CISK mechanisms than their spiral-form North Atlantic counterparts.

By 21.30, the comma cloud stretched between 16 and 22°E and later (02.00, Fig. 1, bottom) the vortex had reached 25°E with a central pressure of 994 hPa and began slowing to 20 m s^{-1}. Rapid occlusion then followed as the comma cloud moved to the east of 25°E. The cloud mass grew beyond mesoscale dimensions (800 km diameter) and the vortex filled rapidly, appearing to outrun its upper support during 5 May as the wave flattened (Fig. 4). Thus rapid cyclogenesis was confined to an area southwest of Cape Town (36°S, 16°–19°E) between the hours of 14.00 and 20.00 on 4 May 1987.

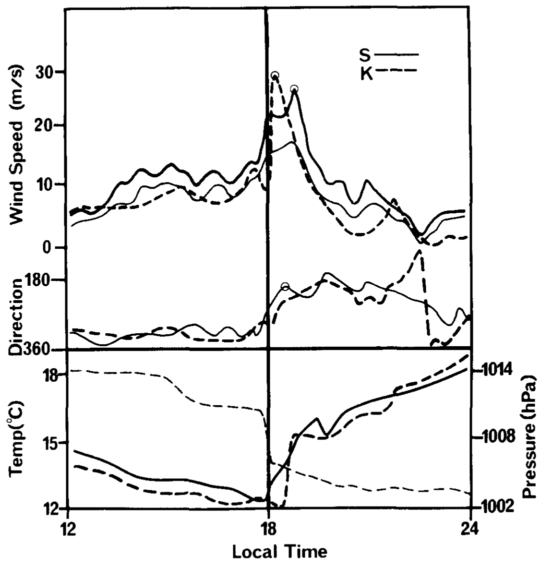

Fig. 9. Time series plots of the wind speed (top), direction (middle) and pressure and temperature (bottom) from digital averages recorded by high response sensors at stations K (dashed) and S (solid), (see Fig. 6). Peak gusts are denoted by open circles and coincide with a sudden rise in pressure.

5. Mesoscale coastal environment

The mesoscale circulation features associated with the meso low–high pair are described in this section using coastal observations (Figs. 1, 5, 6 and 9). Rainfall during the passage of the low was not particularly intense. Line thunderstorms were reported (a local rarity) and rainfall rates for stations near Cape Town (K in Fig. 6) of 5 mm/15 min and 30 mm/12 h were recorded. The highest rainfall rates on the west coast were recorded concurrently with a meso-high/gust front which moved through the area as shown in Fig. 6. Much of the remaining total rainfall was contributed by banded squall lines in the cold sector of the occluded low. These rainfall figures together with the satellite imagery, indicate that the convection was not that well organized or sustained on the coastal side of the meso-low. From the satellite imagery, we would expect higher rainfall rates on the southeast side of the meso-low, outside the coverage of the coastal network. Rainfall totals remained below 30 mm/12 h at coastal stations further east as the low tracked out to sea, leaving the south coast to the east of 25°E relatively unaffected.

Cape Town radiosonde profiles of temperature, dewpoint and wind for 14.00, 4 May 1987, and 02.00, 5 May 1987, are shown in Fig. 5. Prior to cyclogenesis and passage of the storm, winds were from the northwest, reaching 25 m s^{-1} at the 700 hPa level. This is in agreement with the calculated thermal wind value obtained from the 850 hPa isotherm analysis (Fig. 3b) and also meets the requirements of Rogers and Bosart (1986) for concentrated moist, low level inflow (900 hPa, T_d dep = 2°C). Winds at the 200 hPa level reached 70 m s^{-1}, indicating the passage of a jet streak, coincident with the leading edge of the eastwards moving trough. A weak temperature inversion was evident near the 850 hPa level, acting to vertically trap the moisture, while the N–S plateau topography along the west coast channelled the moist inflow into the warm sector. The mid-troposphere was particularly moist as indicated by the very low dewpoint depressions above 600 hPa. Following the passage of the meso-low, a sharp change in wind directions (from 320 to 240°) was evident from the 02.00 profile. Wind speeds below the 500 hPa level abated considerably. Above the inversion at 500 hPa at 02.00, winds were sustained and post-frontal conditions were drier in comparison.

Using time series for stations K and S along the coast, we describe the coastal weather phenomena associated with the passage of the low in Fig. 9. Pressures exhibited step-like falls down to a low value of 1002 hPa by 18.00 on 4 May 1987. A sudden 6 to 8 hPa rise in pressure from 18.00 to 20.00 was recorded immediately following the passage of a gust front, a pattern strikingly similar to that exhibited by the October 1987 storm off the coast of England (Reynolds, 1988). Evidence for a meso-high was supported by the dry slot (Figs. 7 and 8) and by an organized, eastward-propagating humidity minimum recorded in the coastal network, indicative of subsidence following the gust front. Emanuel (1983) discusses aspects of dry roll circulations within frontal rain bands which appear similar to this case. Wind data for west coast and interior locations indicated a sudden swing from northwesterly flow to southwesterly at the same time that speeds increased in association with the east-southeast moving gust front. The gust front had a NE–SW orientation, and slowed and underwent a gradual cyclonic (clockwise) rotation between stations L and S on the west coast near Cape Town. Further eastwards along the south coast, the gust front regrouped and passed over the oil rig at 23.00.

Detailed coastal 10 m wind data were available for stations L, K, S and the oil rig (plots for K and S were shown in Fig. 9). Table 2 summaries this information on peak winds.

A peak gust of 49.1 m s^{-1} was recorded at station K which represents the second highest surface wind speed measured on the African continent. Further into the life history of the storm, at 23.00, winds of 42 m s^{-1} from 260° and heavy rain squalls were observed at the oil rig (position shown in Fig. 6). The strong winds were spatially confined and short lived as indicated by the time series data. In most squall line environments, an intense downburst induces high surface wind speeds which are ageostrophic. However these are accompanied by rainfall rates considerably higher than observed here (Petterssen, 1969). It is therefore likely that the meso-high, rapidly advancing onto the back of the deepening low, caused a more geostrophic flow field with dry dynamics and lower vertical velocities prevailing. The propagation speed of the gust front was estimated as 30 m s^{-1} along the west coast. On the south coast the gust front moved with the leading edge of the occluded low at a speed of 24 m s^{-1}, suggesting that the multiple vortex structure had been consumed.

Table 2. *Coastal wind data during cyclogenesis*

Station	Speed (m s^{-1})	Direction	Time
L	23.7	249°	17.45 hrs
K	38.8	254°	18.15 hrs (49.1 m s^{-1} at 35 m)
S	25.9	224°	18.45 hrs
rig	42.0	260°	23.00 hrs (at 73 m)

The influence of the meso-high is highlighted in Fig. 9 by the rapid anti-clockwise change in wind directions around 22.00. Following a period of calm conditions, representing the centre of the meso-high, westerly flow was resumed at most locations by 24.00. The zonal extent of the meso-high, as deduced from pressure data for stations K, S, and others not shown, is 200 km. The meso-high moved through the area in two hours at a speed of 30 m s^{-1}. The high was thus about one third the size of the developing low. The meso-high had a limited lifespan and no south coast stations reported sudden rises in pressure coincident with the gust front. Perhaps the meso-high was disrupted by the topography and entrained into the occluding vortex.

The coastal data have distinguished certain contrasts in the mesoscale environment over the west and south coasts as a result of different boundary layer forcing and storm structure and movement. The polewards advance of a meso-high during cyclogenesis created a pressure gradient along the west coast estimated at 1 hPa 20 km^{-1}. As the vortex intensified, accelerated and occluded, sweeping along the southern fringe of the African plateau, the meso-high collapsed but gale force winds were maintained along the south coast by the mature low.

6. Summary

The development of a sub-synoptic scale vortex to the southwest of Cape Town on 4 May 1987 has been investigated. In determining the origin of cyclogenesis, attention was focused on both the upper baroclinic forcing and surface heat fluxes. Many of the precursor ingredients cited by other authors for marine cyclogenesis were met by this case study storm. A 70 m s^{-1} jet streak on the leading edge of the upper trough and a diffluent region downstream provided the necessary upper vorticity and divergence patterns for development. In the lower troposphere, moisture convergence was apparent along an axis paralleling the west coast. Surface heat fluxes averaged 200 W m^{-2} across the warm sector of the storm overlying the warm Agulhas Current. Sensible heat fluxes in this case study were about half that of Danard (1986), but latent heat fluxes were larger owing to the high SSTs found within the Agulhas region. The overall SST structure (Fig. 6) closely matched the 850 hPa temperature field (Fig. 3b). The result was that high surface heat fluxes were briefly sustained at the leading edge of the developing baroclinic system, thereby enhancing cyclogenesis through the thermal advection feedback process modelled and discussed by Nuss and Anthes (1987), Atlas (1987), and Wash et al. (1988). It would appear from the limited data set that baroclinic mechanisms were dominant in the rapid intensification (-8 hPa 6 h^{-1}) and acceleration (12 to 24 m s^{-1}) of the low near Cape Town. Satellite imagery of the cyclogenesis stage illustrated the entrainment of a dry slot of air from the equatorwards sector of the storm. The dry slot signified the edge of a meso-high pressure cell advancing onto the northwest side of the deepening low, causing surface winds of over 40 m s^{-1} along the coast.

The rapid eastward movement and intensification of this frontal wave was not anticipated by local forecasters, though in retrospect, the ECMWF model products gave some indication that the necessary upper level precursors were in place. This account of the sub-synoptic scale environment establishes some guidelines for the prediction of marine cyclogenesis in the Cape Town region, as do the studies by Van Heerden (1985) and Triegaardt and Terblanche (1988). Further work on the influence of the spatial distribution of heat fluxes on cyclogenesis and upper ridge enhancement is necessary. It may be useful to interface real-time analyses of surface heat fluxes with ECMWF forecast analyses to provide an index for cyclogenesis near Cape Town. In this context, microwave remote sensing inputs will likely provide significant improvements in data quantity and quality over remote ocean areas of the southern hemisphere in the 1990s. Aircraft surveys can then be used to fill the data gaps left by the coastal and remote sensing data sets, providing an adequate coverage of mesoscale storms which develop to the south of Africa.

7. Acknowledgements

Data for this case study analysis were provided by the S. A. Weather Bureau, Eskom: (station K), the Centre for Scientific and Industrial Research (CSIR): (SST imagery, station S and the oil rig) and from the Department of Agriculture. The Satellite Applications Centre, CSIR is thanked for NOAA imagery.

REFERENCES

Agee, E. M. and Lidrbauch, J. J. 1989. An observational case study of a continental mesoscale vortex. *Tellus 41A*, 222–245.

Atlas, R. 1987. The role of oceanic fluxes and initial data in the numerical prediction of an intense coastal storm. *Dynam. Atm. Oceans 10*, 359–388.

Australian Bureau of Meteorology, 1987. *Climate Monitoring Bulletin, Southern Hemisphere 6*, Melbourne, Australia, 12 pp.

Auer, A. H. 1987. An observational study of polar air depressions in the Australasian region. *Proc. 2nd Int. Conf. S. Hem. Meteor.*, American Met. Soc., Wellington, New Zealand, 46–50.

Bosart, L. F. 1981. The President's Day storm of 18–19 February 1979, a sub-synoptic scale event. *Mon. Wea. Rev. 109*, 1542–1566.

Bratseth, A. 1985. A note on CISK in polar air masses. *Tellus 37A*, 403–406.

Browning, K. A. and Monk, G. A. 1982. A simple model for the synoptic analysis of cold fronts. *Quart. J. Roy. Meteor. Soc. 108*, 435–452.

Businger, S. 1985. The synoptic climatology of polar low outbreaks. *Tellus 37A*, 419–432.

Businger, S. 1987. The synoptic climatology of polar low outbreaks over the Gulf of Alaska and the Bering Sea. *Tellus 39A*, 307–325.

Businger, S. and Walter, B. 1988. Comma cloud development and associated rapid cyclogenesis over the Gulf of Alaska: a case study using aircraft and operational data. *Mon. Wea. Rev. 116*, 1103–1123.

Buzzi, A. and Speranza, A. 1983. Cyclogenesis in the lee of the Alps. In: *Mesoscale meteorology, theories, observations and models* (eds. D. K. Lilly and T. Gal-Chen). Dordrecht: D. Reidel Publ., 55–142.

Callaghan, J. 1987. Subtropical cyclogenesis off Australia's east coast. *Proc. 2nd Int. Conf. S. Hem. Meteor.*, American Meteor Soc., Wellington, New Zealand, 38–42.

Danard, M. 1986. On the sensitivity of predictions of maritime cyclogenesis to convective precipitation and sea temperature. *Atmos. Ocean Dyn. 24*, 52–72.

Davis, C. A. and Emanuel, K. 1988. Observational evidence for the influence of surface heat fluxes on maritime cyclogenesis. *Mon. Wea. Rev. 116*, 12, 2649–2659.

Emanuel, K. 1983. Conditional symmetric instability: a theory for rainbands within extratropical cyclones. In: *Mesoscale meteorology, theory, observations and models* (eds. D. K. Lilly and T. Gal-Chen). Dordrecht: D. Reidel Publ., 231–245.

Emanuel, K. 1986. An air–sea interaction theory for tropical cyclones, part 1, steady state maintenance. *J. Atmos. Sci. 43*, 585–604.

Friehe, C. and Schmitt, K. 1976. Parameterisation of air–sea fluxes of sensible heat and moisture by the bulk aerodynamic formulae. *J. Phys. Oceanogr. 6*, 801–809.

Gilloly, J. F. and Walker, N. D. 1984. Spatial and temporal behaviour of sea surface temperatures in the South Atlantic. *S. A. J. Sci. 80*, 97–100.

Gyakum, J. R. 1983. On the evolution of the QE 2 Storm, 1: synoptic aspects. *Mon. Wea. Rev. 111*, 1137–1155.

Harrold, T. W. and Browning, K. A. 1969. The polar low as a baroclinic disturbance. *Quart. J. Roy. Met. Soc. 95*, 710–723.

Holflich, O. 1984. Climate of the South Atlantic Ocean. In: *Climates of the oceans* (ed. H. VanLoon). *World survey of climatology 15*. Elsevier: Amsterdam, 716 pp.

James, I. N. 1983. Some aspects of the global circulation of the atmosphere in January and July 1980. In: *Large-scale dynamical processes in the atmosphere* (eds. B. J. Hoskins and R. P. Pearce). Academic Press: London, 5–27.

Locatelli, J. O., Hobb, P. V. and Werth, J. A. 1982. Mesoscale structures of vortices in polar air streams. *Mon. Wea. Rev. 110*, 1417–1433.

Mansfield, D. A. 1974. Polar lows, the development of baroclinic disturbances in cold air outbreaks. *Quart. J. Roy. Meteor. Soc. 100*, 541–554.

Murty, T. S., McBean, G. A. and McKee, B. 1983. Explosive cyclogenesis over the NE Pacific Ocean. *Mon. Wea. Rev. 111*, 1131–1135.

Newton, C. W., ed. 1972. *Meteorology of the Southern Hemisphere*, Meteorol. Monogr. *13*, American Meteor. Soc., Boston.

Nuss, W. A. and Anthes, R. A. 1987. A numerical investigation of low level processes in rapid cyclogenesis. *Mon. Wea. Rev. 115*, 2728–2743.

Petterssen, S. V. 1969. *Introduction to Meteorology*. Academic Press: New York.

Rasmussen, E. 1979. The polar low as an extra-tropical CISK disturbance. *Quart. J. Roy. Meteor. Soc. 105*, 531–549.

Rasmussen, E. 1985. A case study of a polar low development over the Barents Sea. *Tellus 37A*, 407–418.

Rasmussen, E. and Zick, C. 1987. A sub-synoptic scale vortex over the Mediterranean with some resemblance to polar lows. *Tellus 39A*, 408–425.

Reed, R. J. 1979. Cyclogenesis in polar airstreams. *Mon. Wea. Rev. 107*, 38–52.

Reed, R. J. and Albright, M. D. 1986. A case study of explosive cyclogenesis in the eastern Pacific. *Mon. Wea. Rev. 114*, 2297–2319.

Reynolds, R. 1988. A chronicle of the storm of 15 and 16 October 1987. *NERC News*, Wiltshire: England.

Rogers, E. and Bosart, L. F. 1986. An investigation of explosively deepening oceanic cyclones. *Mon. Wea. Rev. 114*, 702–718.

Sanders, F. 1986. Explosive cyclogenesis in the west-central North Atlantic Ocean, 1981–84, part 1: composite structure and mean behaviour. *Mon. Wea. Rev. 114*, 1781–1794.

Sardie, J. M. and Warner, T. T. 1983. On the mechanism for the development of polar lows. *J. Atm. Sci. 40*, 869–881.

Shapiro, M. A., Fedopr, L. S. and Hampel, T. 1987. Research aircraft measurements of a polar low over the Norwegian Sea. *Tellus 39A*, 272–306.

Triegaardt, D. O. and Terblanche, D. E. 1988. A case study of a rapid cyclogenesis over Southern Africa on 2 September 1988. *S. A. Wea. Bureau Newsletter 474*, 1–4.

Van Heerden, J. 1985. Analysis of the 1000–300 hPa thickness field using satellite imagery. *S. A. Wea. Bureau Tech. Rep. 15*, 27 pp.

Wallace, J. M. 1983. The climatological mean stationary waves: observational evidence. In: *Large-scale dynamical processes in the atmosphere*, Academic Press: London, 27–55.

Wash, C. H., Peak, J. E., Calland, W. E. and Cook, W. A. 1988. Diagnostic study of explosive cyclogenesis during FGGE. *Mon. Wea. Rev. 116*, 431–451.